

Spatial and temporal variation in thaw depth in Siberian tundra near Tiksi

K. Watanabe & H. Kiyosawa

Faculty of Bioresources, Mie University, Tsu, Japan

K. Fukumura

Department of Environmental Engineering, Utsunomiya University, Utsunomiya, Japan

T. Ezaki

Fujita Corporation, Tokyo, Japan

M. Mizoguchi

Department of Biological and Environmental Engineering, The University of Tokyo, Tokyo, Japan

ABSTRACT: Siberian tundra is characterised by permafrost overlaid with an active layer. The spatial and temporal variation in the thaw depth in the active layer may play an important role in biological and hydrological processes. In this study, we carried out field investigations of flat tundra and a hillslope in a watershed near Tiksi, Siberia, at various scales, from 1997 to 2000. The ground started to thaw in early June and refroze in mid September. The progress in the ground thaw was proportional to the square root of the thawing index. The maximum thaw, which was observed at the end of August, ranged from 1.2 to 0.2 m and averaged 0.4 m. The spatial variation was analysed using a variogram method. The ground thaw had a fractal dimension ($=1.8$) at each scale. While there was no anisotropy in the thaw depth in the flat area, the thaw depth on the hillslope periodically fluctuated perpendicular to direction of maximum slope.

1 INTRODUCTION

Siberian tundra is characterised by permafrost overlaid by a thin layer that freezes and thaws annually, the active layer. Almost all the biological and hydrological processes in the tundra occur on or within the active layer (Hinzman et al. 1991, 1998). In tundra regions, the flux of greenhouse gases, such as CO₂ and CH₄, are related to the thaw depth and moisture condition of the active layer (Kane et al. 1991, Vourlitis et al. 1993). The thaw and freeze dynamics of the active layer influence the hydrology, hydrogeology, and geomorphology of the tundra (Hinzman et al. 1991, Hinzman & Kane 1997, Watanabe et al. 2001). Monitoring variation in the active layer thaw is necessary for assessing changes in the environment.

The thaw depth in the active layer can vary substantially over short distances and time periods because heat transfer in soils that are subject to freezing and thawing reflects the interaction of a large number of highly localised factors, including vegetation type, snow cover, organic layer thickness, soil thermal properties, soil moisture, microtopography, and the operation of nonconductive heat-transfer processes (Washburn 1980, Outcalt et al. 1990). To measure thaw depth with maximum effectiveness, the spatial representation and optimal interval of measurement sites must be considered. It is important to obtain quantitative estimates of the variability in the thaw depth in the active layer. Few examples of such work are available for the Siberian tundra however. The

primary goal of this study was to describe the spatial and temporal variation of thaw depth in the active layer of a Siberian tundra watershed. Such information forms an important component of any strategy attempting to integrate observations into a regional overview.

2 STUDY AREA

The study area was located in a typical tundra watershed (Walker et al. 1998), situated 5 km southwest of Tiksi, Russia (latitude 71°38'N, longitude 128°52'E) (Fig. 1). The topography of this watershed consists of rolling hills, with gently sloping hillslopes and elevations of 200–300 m. Marshy wetlands develop at the bottom of these slopes. The vegetation mainly consists of water-tolerant plants, such as sedges (*Carex* sp. and *Eriophorum* sp.) and mosses (*Sphagnum* sp., *Aulacomnium* sp., *Calliergon* sp., *Dicranum* sp., and *Polytrichum* sp.), accompanied by lichens (*Cetraria* sp., *Alectoria* sp., and *Dryas* sp.) and low shrubs (*Salix* sp.). The soil is a multi-layered system that consists of 0–0.2 m of live and accumulated organic material on 0.05–0.3 m of partially decomposed organic matter, which overlies a mineral silt above the bedrock (Watanabe et al. 2000). The hydraulic conductivity of the organic soils is 10 to 100 times greater than that of the silt.

The live-plant layer of moss has a very high conductivity.

The thermal conductivity increases with depth from the live-plant layer through the organic soil to the silt (Watanabe et al. 2000). The hilltops are covered by shale, with some lichens (*Umbilicaria* sp., *Rhizocarpon* sp., *Dryas* sp., *Festuca* sp., and *Luzula* sp.). The permafrost is estimated to be over 500 m thick (Fartyshev 1993). A network of ice-wedge polygons with diameters of about 7 m occur in the tundra. A field of these polygons was studded with non-sorted circles (*frost boils*) about 0.5 m in diameter (Washburn 1980).

This survey was carried out between 1997 and 2000. The average air temperature was -13.5°C , with a maximum recorded temperature of 32.6°C and a minimum of -53.6°C . The air temperature remained below 0°C from mid September to mid May. The average annual precipitation was 345 mm. Compared to the ground thaw season in 1997, there was less precipitation in 1998 and relatively warmer temperatures in 1999 and 2000. The prevailing winds were northeasterly in summer and southwesterly in winter (Kodama 1998). Due to relatively high wind speeds (mean of 5 m/s), less than 0.1 m of snow accumulated in the wetlands and it piled into drifts (2–20 m thick) in the valleys during winter. The drifted snow remained until August, and supplied water for the wetlands.

3 METHODS

An area of $1000\text{ m} \times 1000\text{ m}$, consisting of a network of 121 precisely located permanent stakes, driven into the permafrost at 100 m horizontal intervals (F100G), was established in a tundra flat (Hinzman 1997). Nested (hierarchical) square grids with intervals of 10, 5, and 1 m were fitted inside the southeast end of the area (F10G, F5G, F1G) (Fig. 1). A meteorological station was located 100 m south of the area. Parts of the area were covered by a mat of moss forming a 0.03–0.2 m layer of live plants. Likewise, an area of $100\text{ m} \times 100\text{ m}$ was chosen on a hillslope (average gradient 2°), and nested grids with intervals of 10, 5, and 1 m were set up in the area (S10G, S5G, S1G).

The thaw depth of the ground was measured monthly at each grid intersection from June to September using a steel rod, calibrated in centimetres and pushed vertically into the ground. Since it was difficult to recognise the ground surface where it was covered by a thick mat of moss, we placed a wooden panel ($0.2\text{ m} \times 0.2\text{ m}$, weight 500 g) on the plants and set this as the ground surface. Mackay (1995) discusses some potential sources of error associated with this methodology. Soil temperatures were measured at depths of 0.1 and 0.2 m using a thermistor, and the thaw depth was checked every August. In August, the ground surface level, ground water level, gradient, soil type, and soil moisture were also investigated at each intersection.

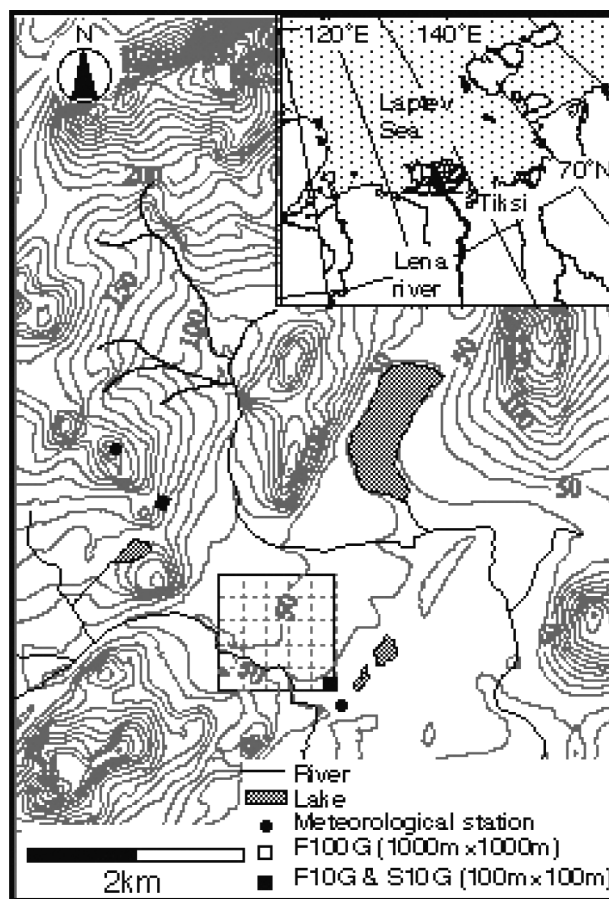


Figure 1. Study area. (10 m contour interval.)

Additionally, the vegetation cover in each 10 m square grid was classified by the dominant species observed (Watanabe et al. 2001).

4 RESULTS AND DISCUSSION

4.1 Temporal variation in thaw depth

4.1.1 Difference by year

Table 1 lists the thaw depth in each grid during the maximum thaw season between 1997–2000 (i.e. active layer thickness). The average thaw was $0.40 \pm 0.15\text{ m}$ and the maximum and minimum values were 1.05 m and 0.15 m, respectively. Compared with 1997, the ground thaw was shallower in 1998, as a result of a dry summer, and deeper in 1999 and 2000, which were warmer summers. A similar trend was not seen in the maximum and minimum values of thaw depth however (Table 1).

Ground thaw is strongly influenced by the properties of vegetation and soil (Nelson et al. 1997, 1999, Hinkel et al. 2000). In this watershed, thaw depth varies with vegetation type, the vegetation cover ratio and micro-undulations, which induce water runoff (Watanabe et al. 2001). Figures 2a–c map the thaw depth in F10G in

1997, 1998, and 1999, respectively. The ground thawed to a deeper level in the northwestern part of the grid than in the southeastern part. At some points near the northwestern midpoint of the grid, the thaw

Table 1. Active-layer thickness in the observation grid.

year	day	N	Avg		Std		Cov (%)
			(cm)	max	min	(cm)	
10 m × 10 m, 1 m interval (F1G)							
1997	8/15	625	35.1	48	25	4.79	13.65
1998	8/17	625	55.4	72	35	7.29	13.16
100 m × 100 m, 10 m interval (F10G)							
1997	8/16	121	56.1	105	27	15.90	28.34
1998	8/15	121	49.9	100	25	14.93	29.91
1999	8/19	121	60.7	102	29	15.69	25.85
1000 m × 1000 m, 100 m interval (F100G)							
1997	8/22	121	40.6	84	18	13.02	32.07
1998	9/12	121	40.2	81	25	10.01	24.90
1999	9/18	121	41.6	79	15	11.07	26.61
2000	8/26	121	45.2	75	26	10.74	23.78

N indicates number of samples; Avg, Std and Cov are average, standard deviation and coefficient of variance.

depth was close to 1 m. The thaw depth was locally deeper at or near water-filled depressions and near non-sorted circles. It was shallower in moss-covered areas. The locations of points at which the ground thaw was deeper were similar in all three years, as were the depth of thaw, despite the year-to-year spatial variation in the thaw and mean thaw depth.

4.1.2 Seasonal change

The soil in the observation area started to thaw in mid June, reaching a maximum depth in late August to early September, before refreezing after mid September. Several previous studies have addressed the correlation between thaw depth and air temperature records (e.g. Gray et al. 1988, Jorgenson & Kreig 1988). Figure 2 shows the seasonal change in the average thaw depth and the standard deviation at F10G and S10G in 1998. The thawing index is a time-temperature integral, calculated by summing the mean daily temperatures above 0°C (Harlan & Nixon, 1978). In both observation grids, the ground thaw progressed as the thawing index increased, and reached its maximum depth in late August. The average thickness of the active layer was

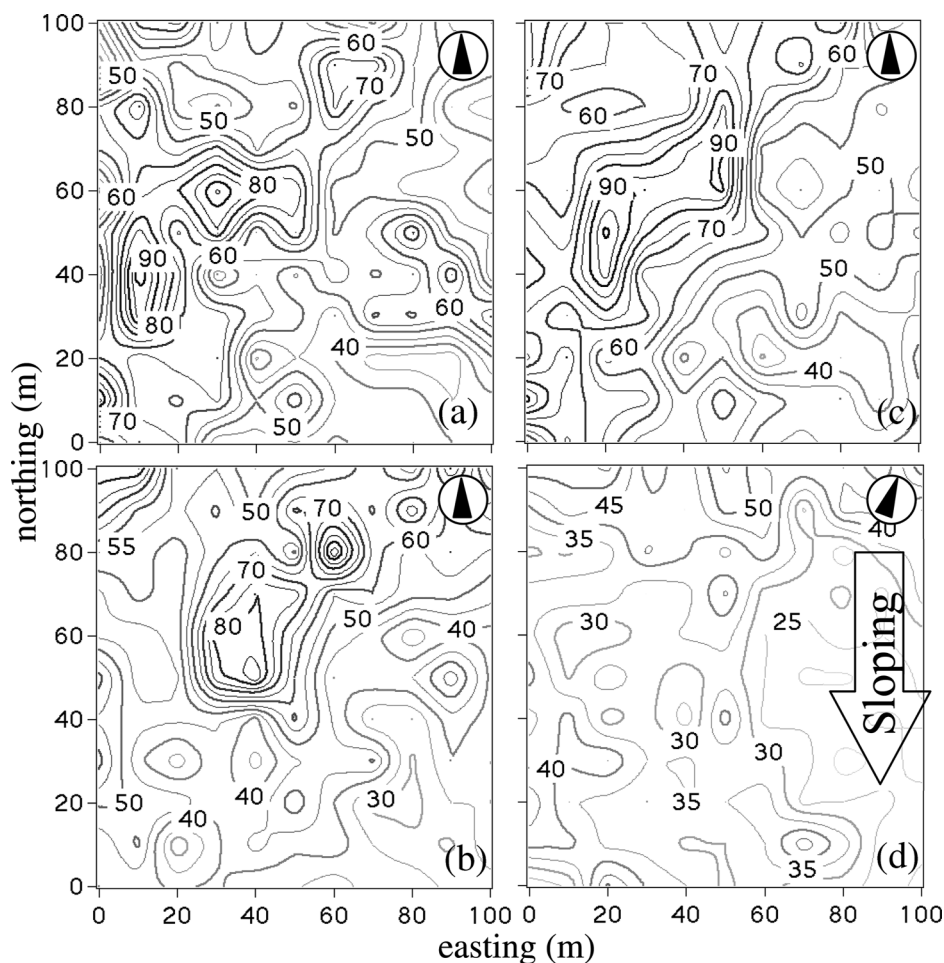


Figure 2. Maps of thaw depth in the 100 m × 100 m observation area on flat tundra, F10G (a–c), and hillslope, S10G (d). (a) August 16, 1997; (b) August 15, 1998; (c) August 19, 1999; (d) August 20, 1998. The solid lines are the thaw depth contour with a 5 cm interval.

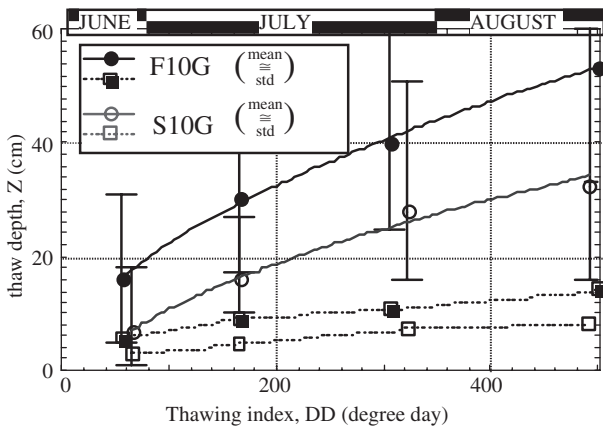


Figure 3. Seasonal change in thaw depth in the 100 m × 100 m observation area on the flat tundra (F10G) and hillslope (S10G) in 1998.

53.5 cm in F10G (range 33 to 83 cm) and 32.6 cm in S10G (range 16 to 60 cm). The standard deviation increased with increasing thaw depth, indicating that variation increased as the ground thawed.

The relationship between thaw depth, Z , and the thawing index, DD , was $Z_{F10G} = 1.9 DD^{0.54}$ ($R^2 = 0.99$) for F10G and $Z_{S10G} = 2.0 DD^{0.53} - 8.5$ ($R^2 = 0.99$) for S10G (shown as solid lines in Fig. 3). In both areas, the ground thaw was roughly proportional to the square root of the thawing index, indicating that the trend in the seasonal change in thaw depth in this watershed is primarily homogeneous. These relationships agree with the form of the Stefan solution, which has been used in studies of active layer thickness (e.g. Hinkel & Nicholas 1995, Nelson et al. 1997). The active layer on the hillslope was shallower than that on the tundra flat, despite similar air temperatures and vegetation. This was presumably due to differences in slope aspect and the existence of a snow patch just above the hillslope, which continually supplied flowing cold water to S10G during the ground-thaw season.

4.2 Spatial variation in thaw depth

4.2.1 Topography

The depth of thaw differed between the tundra flat and hillslope, although the trend in ground thaw progression was similar at the two sites (Fig. 3). We analysed the spatial variability in both observation grids (F10G & S10G). Figures 2b and 2d map the thaw depth in F10G and S10G respectively, in the maximum thaw season of 1998. S10G was oriented in the direction of the slope. The average thaw depth was deeper in F10G than in S10G. In F10G, locally deep thaws were observed near non-sorted circles, which consisted of silt with a high thermal conductivity. This factor was compounded by the lack of vegetation on their surface and a reduced albedo. Dense contour lines are therefore

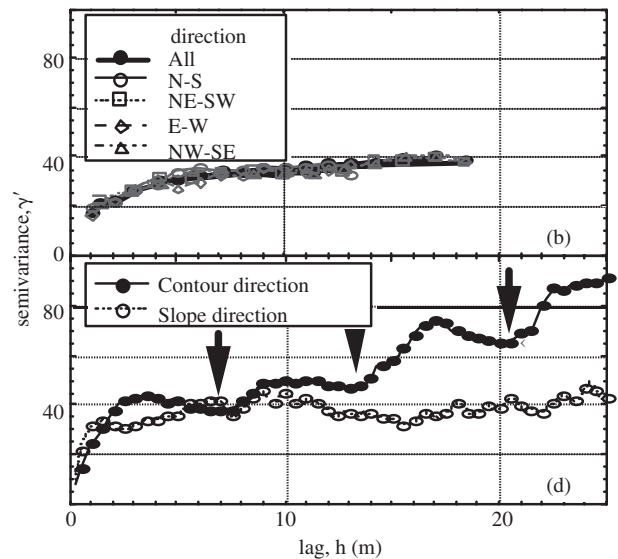


Figure 4. Semivariogram for F10G (b) and S10G (d).

seen in the thaw-depth map. By contrast, no non-sorted circles were observed in S10G. Numerous water tracks developed into gullies in the hillslope. In some places, the active layer in these gullies was deeper than that on the tundra flat.

The spatial correlation in thaw depth variation was calculated by semivariogram, $\gamma' = 0.5 \text{ var}\{z(s+h) - z(s)\}$, where z is the thaw depth at point s , and h is the spatial lag. The spatial variation increases with γ' . If anisotropy were present, γ' has a different form (Mizoguchi et al. 1998, Gomersall & Hinkel 2001). Figures 4b and 4d show γ' for F10G and S10G, respectively, associated with each lag distance. In F10G, γ' flattens at a lag of about 10 m (range ≈ 10 m), indicating that sampling of thaw depth at intervals over 10 m are independent observations. No difference in γ' was observed in any direction. There appears to be no anisotropy in the thaw depth in the tundra flat. Likewise, no periodicity of γ' was detected for the slope direction in S10G. By contrast, γ' for the contour direction in S10G had local minima with a periodicity of 7 m (arrows in Fig. 4d). Water tracks meandered through the surface of ice wedges that formed at an angle around the polygons, and some of the water tracks developed into gullies. Although the ground thaw is mainly dependent on the vegetation and the thermal properties of soil (Nelson et al. 1997, 1999, Hinkel et al. 2000, Watanabe et al. 2001), γ' observed in the contour direction may be attributed to the water tracks. The drop in periodicity in the direction of the slope can be explained in terms of movement of the subsurface soil by solifluction.

4.2.2 Scale

The values of thaw depth, such as average and maximum thaw, differed when a different grid interval was

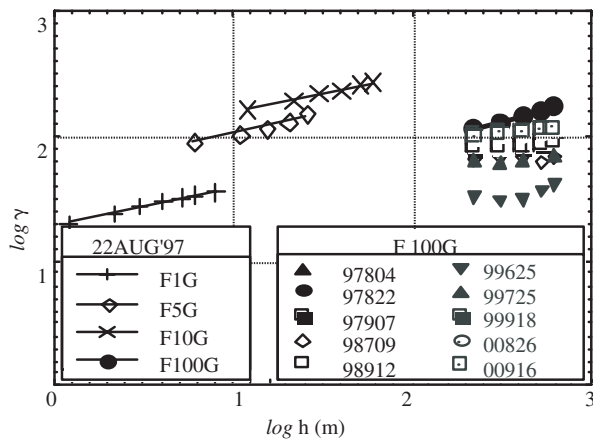


Figure 5. Variogram for each scale.

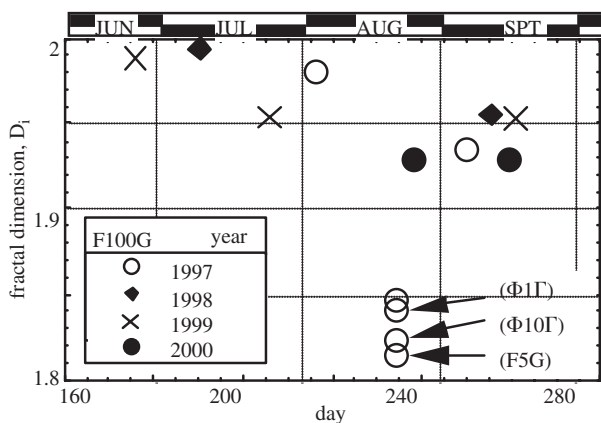


Figure 6. Fractal dimension for each observation area on flat tundra.

selected (Table 1). The difference between the maximum and minimum thaw depth decreased, and detailed variation in thaw depth was obscured by increasing the grid interval. Here, we compare the spatial variability for each grid size. Figure 5 shows the relationship between variogram, γ , and the lag, h , for each scale (F1G, F5G, F10G, & F100G) in the maximum thaw season of 1997, and for F100G during the 1997–2000 thaw seasons. There are no fundamental differences in the variability of thaw depth at each grid scale, which have similar fractal dimensions, D_i ($4-2 D_i = \Delta \log \gamma / \Delta \log h \approx 0.33$; $D_i = 1.8$) (Burrough 1981, Zhang et al. 2001). Figure 6 shows the seasonal change in the fractal dimension observed in Figure 5. The fractal dimension decreased with ground thaw, reached a minimum value during the maximum ground thaw period, and then increased with ground freezing, presumably because ground thaw progressed irregularly during the first stage, becoming smooth as it progressed. A similar trend was observed in all observation years. Although the D_i value is high, it would seem worthwhile to use the D_i value as a guide to further mapping and observation.

These results suggest the optimal sampling interval for field observations in this watershed. Figures 5 and 6

show that an interval of 100 m or greater is adequate for capturing the primary scale of the variability in ground thaw for this watershed. This interval fails however to resolve some of the minor variability related to localised phenomena. At the scale of hydrological processes associated with cryogenic topography such as gully erosion and solifluction, sampling at less than 10 m intervals is useful, as shown in Figure 4. Alternatively, to consider the specific mechanism of ground thaw at one point, we may need to determine the soils' thermal properties, surface conditions, and vegetation cover at a spatial interval that is at least the same as that used for the maximum thaw depth (i.e. 1 m or less for this watershed) (Watanabe et al. 2001).

5 CONCLUSION

Variability in thaw depth occurred at different temporal and spatial scales in a tundra watershed near Tiksi, Siberia. The ground began to thaw in early June and refroze in mid September. The progression of ground thaw was proportional to the square root of the thawing index. The maximum thaw, which was observed at the end of August, ranged from 1.2–0.2 m and averaged 0.4 m. While there was no anisotropy in the variance of thaw depth in the tundra flat, the thaw depth on the hillslope periodically fluctuated perpendicular to the gradient. The ground thaw had a similar fractal dimension (≈ 1.8) that was independent of the sampling interval. Although temporal and spatial variations in thaw depth are important for understanding biological and hydrological interactions, it is difficult to identify the variation in a large watershed over a short time. Our results have significant implications for designing effective strategies for the sampling and construction of regional estimates of thaw depth and closely related phenomena.

ACKNOWLEDGMENT

This work was supported by the Japanese GAME Siberia Program.

REFERENCES

- Burrough, P.A. 1981. Fractal dimensions of landscapes and other environmental data. *Nature* 294:240–242.
- Fartyshev, A.I. 1993. *Peculiarities of the coastal-shelf cryolithozone of the Laptev Sea*. Novosibirsk: Nauka. (in Russian)
- Gomersall, C.E. & Hinkel, K.M. 2001. Estimating the variability of active-layer thaw depth in two physiographic regions of northern Alaska. *Geographical Analysis* 33: 141–155.

- Gray, J.T., Pilon, J. & Poitevin, J. 1988. A method to estimate active-layer thickness on the basis of correlation between terrain and climatic parameters as measured in northern Quebec. *Canadian Geotechnical Journal* 25:607–616.
- Harlan, R.L. & Nixon, J.F. 1978. Ground thermal regime. In O.B. Andersland & D.M. Anderson (eds), *Geotechnical Engineering for Cold Regions*: 103–163. New York: McGraw Hill.
- Hinkel, K.M. & Nicholas, J.R.J. 1995. Active layer thaw rate at a boreal forest site in central Alaska, USA. *Arctic and Alpine Research* 27:72–80.
- Hinkel, K.M., Nelson, F.E., Bockheim, J.G., Miller, L.L. & Paetzold, R.F. 2000. Spatial and temporal patterns of soil moisture and depth of thaw at proximal acidic and nonacidic tundra sites, north-central Alaska, U.S.. In R. Lal, J.M. Kimble & B.A. Stewart (eds), *Global Climate Change and Cold Regions Ecosystems*: 197–209. Boca Raton: Lewis Publishers.
- Hinzman, L.D., Kane, D.L., Gieck, R.E. & Everett K.R. 1991. Hydrologic and thermal properties of the active layer in the Alaskan arctic. *Cold Regions Science and Technology* 19: 95–110.
- Hinzman, L. D. 1997. CALM grid installation. In *Activity Report of GAME-Siberia, 1996–1997*: 47–49. Japan, Japan sub-Committee for GAME-Siberia.
- Hinzman, L.D. & Kane, D.L. 1997. Measured and modeled Arctic hydrologic processes at the watershed scale. In *Proc. Conference on Polar Processes and Global Climate, Washington, 3–6 November 1997*: 86–88. Oslo, International ACSYS Project Office.
- Hinzman, L.D., Goering, D.J. & Kane, D.L. 1998. A distributed thermal model for calculating temperature profiles and depth of thaw in permafrost regions. *J. Geophysical Research – Atmospheres* 103: 975–991.
- Jorgenson, M.T. & Kreig, R.A. 1988. A model for mapping permafrost distribution based on landscape component maps and climatic variables. In K. Sennesket (ed) *Proc. Fifth Int. Conf. Permafrost vol. 1.*: 176–182. Trondheim: Tapir Publisher.
- Kane, D.L., Hinzman, L.D. & Zarling, J.P. 1991. Thermal response of the active layer to climatic warming in a permafrost environment. *Cold Regions Science and Technology* 19:111–122.
- Kodama, Y. 1998. The outline of the field observations in tundra region in 1998. In *Activity Report of GAME-Siberia, 1998*: 7–12. Japan, Japan sub-Committee for GAME-Siberia.
- Mizoguchi, M., Watanabe, K. & Kodama, Y. 1997. Spatial variation of active layer thickness in Siberian tundra. In *Activity Report of GAME-Siberia, 1996–1997*: 54–56. Japan, Japan sub-Committee for GAME-Siberia.
- Nelson, F.E., Shiklomanov, N.I., Mueller, G.R., Hinkel, K.M., Walker D.A. & Bockheim J.G. 1997. Estimating active-layer thickness over a large region: Kuparuk river basin, Alaska, USA. *Arctic and Alpine Research* 29: 367–378.
- Nelson, F.E., Shiklomanov, N.I. & Muller, G.R. 1999. Variability of active-layer thickness at multiple spatial scale, north-central Alaska, USA. *Arctic, Antarctic and Alpine Research* 31:179–186.
- Outcalt, S.I., Nelson, F.E. & Hinkel, K.M. 1990. The zero-curtain effect: heat and mass transfer across an isothermal region in freezing soil. *Water Resources Research* 26: 1509–1516.
- Vourlitis, G.L., Oechel, W.C., Hastings, S.J. & Jenkins, M.A. 1993. The effect of soil moisture and thaw depth on CH₄ flux from wet coastal tundra ecosystems on the North Slope of Alaska. *Chemosphere* 26:329–337.
- Walker, D.A., Auerbach, N.A., Bockheim, J.G., Chapin III, F.S., Eugster, W., King, J.Y., McFadden, J.P., Michaelson, G.J., Nelson, F.E., Oechel, W.C., Ping, C.L., Reeburg, W.S., Regli, S., Shiklomanov, N.I. & Vourlitis G.L. 1998. Energy and trace-gas fluxes across a soil pH boundary in the Arctic. *Nature* 394: 469–472.
- Washburn, A.L. 1980. *Geocryology*. New York: Wiley.
- Watanabe, K., Mizoguchi, M., Kiyosawa, H. & Kodama, Y. 2000. Properties and horizons of active layer soils in tundra at Tiksi, Siberia. *Journal of Japan Society of Hydrology and Water Resources* 13: 9–16. (in Japanese)
- Watanabe, K., Ezaki, T., Fukumura, K., Mizoguchi, M., & Kiyosawa, H. 2001. Variability of thaw depth depending on surface micro-undulation and vegetation cover in the Siberian tundra. In *Proc. Fifth Intern. Study Conf. GEWEX in Asia and GAME vol. 3, 3–5 October 2001*: 632–636. Nagoya, GAME International Project Office.
- Zhang, X., Drake, N.A., Wainwright, J. & Mulligan, M. 1999. Comparison of slope estimates from low resolution DEMs: scaling issues and a fractal method for their solution. *Earth Surface Processes and Landforms* 24: 763–779.